

Deciphering the Role of Hole Transport Layer HOMO Level on the Open Circuit Voltage of Perovskite Solar Cells

Zhongyao Jiang, Tian Du,* Chieh-Ting Lin, Thomas J. Macdonald, Jiongye Chen, Yi-Chun Chin, Weidong Xu, Bowen Ding, Ji-Seon Kim, James R. Durrant, Martin Heeney, and Martyn A. McLachlan*

With the rapid development of perovskite solar cells, reducing losses in open-circuit voltage (V_{oc}) is a key issue in efforts to further improve device performance. Here it is focused on investigating the correlation between the highest occupied molecular orbital (HOMO) of device hole transport layers (HTLs) and device V_{oc} . To achieve this, structurally similar HTL materials with comparable optical band gaps and doping levels, but distinctly different HOMO levels are employed. Using light-intensity dependent V_{oc} and photoluminescence measurements significant differences in the behavior of devices employing the two HTLs are highlighted. Light-induced increase of quasi-Fermi level splitting (ΔE_F) in the perovskite layer results in interfacial quasi-Fermi level bending required to align with the HOMO level of the HTL, resulting in the V_{oc} measured at the contacts being smaller than the ΔE_F in the perovskite. It is concluded that minimizing the energetic offset between HTLs and the perovskite active layer is of great importance to reduce non-radiative recombination losses in perovskite solar cells with high V_{oc} values that approach the radiative limit.

that are the electron- and hole-transport layers (ETL/HTLs) play an essential role in ensuring contact selectivity, resulting in reduced interfacial recombination and ultimately enhanced open-circuit voltage (V_{oc}) and fill factor.^[6–8] The correlation between interfacial recombination and V_{oc} losses has been widely studied, with photoluminescence (PL) spectroscopy being commonly used as a tool to interrogate recombination.^[9–12]

One pertinent question that remains unanswered relates to the relationship between the highest occupied molecular orbital (HOMO) of the HTL ($HOMO_{HTL}$) and the device V_{oc} . Whilst some studies indicate that V_{oc} is insensitive to $HOMO_{HTL}$ others show a correlation between $HOMO_{HTL}$ and V_{oc} .^[13,14] Such differences can be explained when considering the most commonly reported organic HTLs, for example, poly(3,4-ethylenedioxythiophene) polystyrene sulfonate (PEDOT:PSS), poly(triaryl amine) (PTAA), poly(N,N'-bis-4-butylphenyl-N,N'-bisphenyl)benzidine (PolyTPD) and poly(3-hexylthiophene) (P3HT). In these materials changes in $HOMO_{HTL}$ are accompanied by simultaneous shifts in the lowest unoccupied molecular orbital energy, as well as variations in film morphology, carrier concentrations, and defect densities, which all have an effect on carrier recombination and device V_{oc} . Physicochemical

1. Introduction

Significant research volume has been channeled into controlling and optimizing the structure, composition, and performance of metal-halide perovskite solar cells (PSCs).^[1–5] Such devices are inherently multi-layer systems thus it's critical to consider not only the individual functional layers but additionally their interfaces. Device charge selective interlayers

that are the electron- and hole-transport layers (ETL/HTLs) play an essential role in ensuring contact selectivity, resulting in reduced interfacial recombination and ultimately enhanced open-circuit voltage (V_{oc}) and fill factor.^[6–8] The correlation between interfacial recombination and V_{oc} losses has been widely studied, with photoluminescence (PL) spectroscopy being commonly used as a tool to interrogate recombination.^[9–12]

Z. Jiang, T. Du, C.-T. Lin, M. A. McLachlan
Department of Materials and Centre for Processable Electronics
Molecular Science Research Hub
Imperial College
London W12 0BZ, UK
E-mail: tian.du14@imperial.ac.uk; martyn.mclachlan@imperial.ac.uk

C.-T. Lin
Now at Department of Chemical Engineering
National Chung Hsing University
145 Xingda Rd, South Dist., Taichung 402, Taiwan

T. J. Macdonald, W. Xu, B. Ding, J. R. Durrant, M. Heeney
Department of Chemistry and Centre for Processable Electronics
Molecular Science Research Hub
Imperial College
London W12 0BZ, UK

T. J. Macdonald
School of Engineering and Materials Science
Queen Mary University of London
London E1 4NS, UK

J. Chen, Y.-C. Chin, J.-S. Kim
Department of Physics and Centre for Processable Electronics
Imperial College London
London SW7 2AZ, UK

J. Chen
Quality Testing and Inspection Center of Grid Construction
Now at China Electric Power Research Institute
Beijing 10019, China

 The ORCID identification number(s) for the author(s) of this article can be found under <https://doi.org/10.1002/admi.202201737>.

© 2022 The Authors. Advanced Materials Interfaces published by Wiley-VCH GmbH. This is an open access article under the terms of the Creative Commons Attribution License, which permits use, distribution and reproduction in any medium, provided the original work is properly cited.

DOI: 10.1002/admi.202201737

differences between materials, for example, surface hydrophilicity may also influence the structure and morphology of the perovskite layer deposited on top.^[15] Thus deconvoluting the role of HOMO_{HTL} on device performance is a multi-faceted challenge.

Here, we investigate the origins of the relationship between HOMO_{HTL} and device V_{oc} , by comparing the HTL

performance of poly[bis(4-phenyl)(2,4,6-trimethylphenyl)amine] (PTAA) with that of a related co-polymer, poly[9,9-dioctyl-9H-fluorene-co-bis(4-phenyl)(2,4-dimethylphenyl)amine] (PF8TAA).^[16] Both polymers have similar molecular structures (Figure 1a), comparable optical band gaps and doping levels, but have distinctly different HOMO levels (Table S1, Supporting Information), and when used as HTLs in perovskite PV result

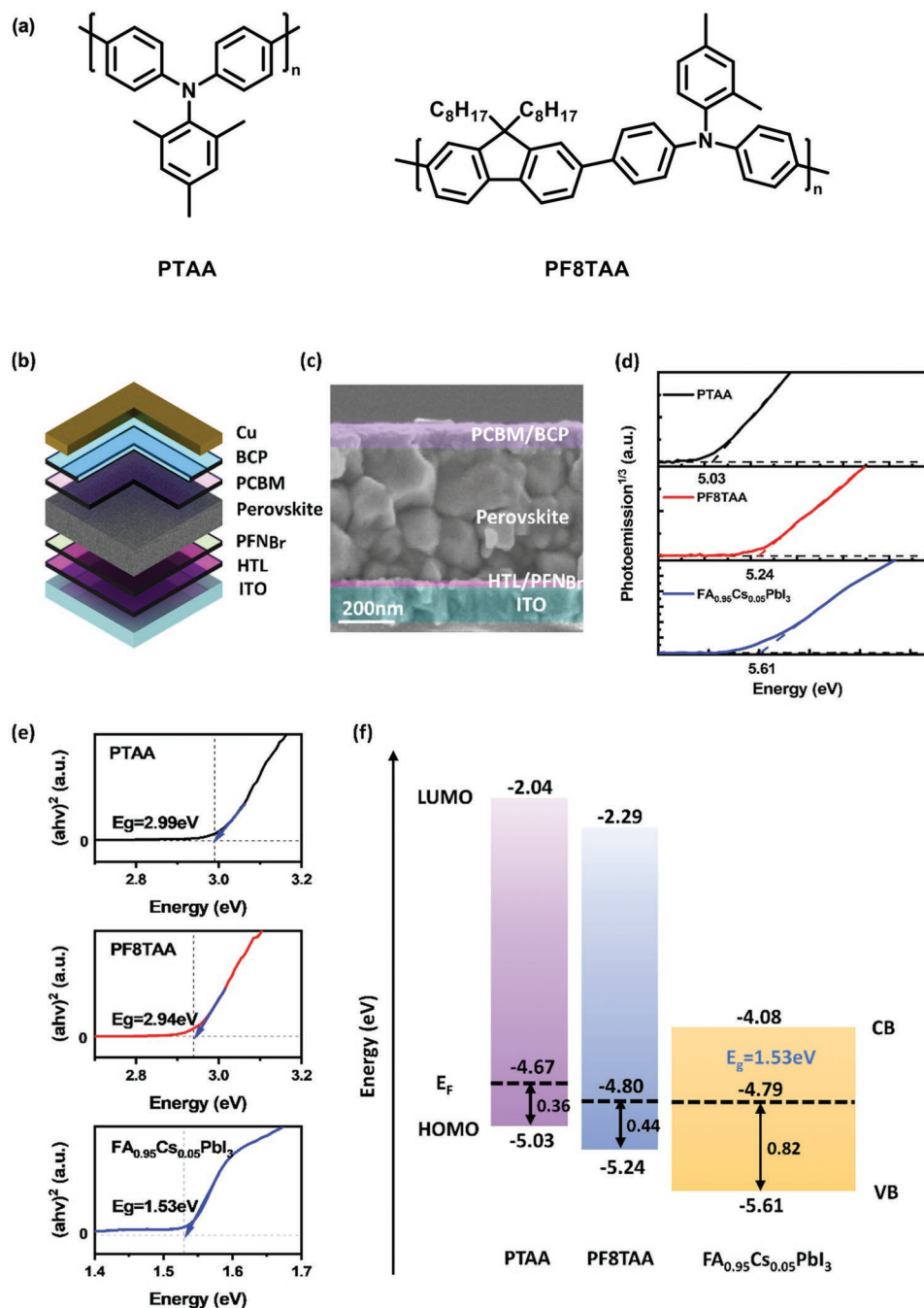


Figure 1. a) The molecular structures of PTAA and PF8TAA. b) Schematic illustration showing the p-i-n device architecture. c) Cross-section scanning electron microscopy (SEM) image of a typical PSC. d) Ambient pressure photoemission spectroscopy (APS) spectra of PTAA, PF8TAA, and FA_{0.95}Cs_{0.05}PbI₃ films (three plots at different X, Y scales). e) Tauc plots from the UV-vis spectra of PTAA, PF8TAA and FA_{0.95}Cs_{0.05}PbI₃ films. f) Flat band energy diagram at the HTL/perovskite interfaces.

in devices with different V_{oc} values. Using light-intensity dependent steady-state PL measurements, we show that the HOMO_{HTL} begins to limit the achievable V_{oc} as light intensity increases. This is shown to be a consequence of increases in the magnitude of the quasi-Fermi level splitting (ΔE_F) in the bulk perovskite resulting in greater upward bending of the hole quasi-Fermi level ($E_{F,p}$) in the HTL.

2. Results and Discussion

A schematic illustration of the device architecture fabricated is shown in Figure 1b. PTAA and PF8TAA HTLs were deposited directly onto indium-doped tin oxide substrates without the addition of any additional co-dopants. An ultrathin layer of poly(9,9-bis(3'-(*N,N*-dimethyl)-*N*-ethylammonium-propyl-2,7-fluorene)-alt-2,7-(9,9-dioctylfluorene))dibromide (PFN-Br) (<10 nm) was deposited onto the HTLs as an amphiphilic surface modifier, to improve the wettability of the HTL surface prior to deposition of the perovskite layer.^[17] The perovskite layers (MAPbI₃/FA_{0.95}CS_{0.05}PbI₃) were deposited via an antisolvent dripping method (full details in Supporting Information). Devices were completed by depositing (6,6)-phenyl-C₆₁-butyric acid methyl ester (PCBM) as the ETL followed by a thin bathocuproine layer and finally upon thermal evaporation of the Cu electrode. A typical device structure is shown in the cross-section scanning electron microscope (SEM) image in Figure 1c. From these images we observe a slight increase in the average grain size when PF8TAA is employed, accompanied also by an increase in the grain dispersity however no global changes in crystallinity were detected, Figure S1 and Table S2 (Supporting Information).

Inspection of the molecular structures of PTAA and PF8TAA, Figure 1a, shows the incorporation of a fluorene unit in the latter that is designed to improve charge carrier mobility.^[16] The HOMO levels of the HTLs are obtained from their ionization potentials (IP), measured using ambient pressure photoemission spectroscopy (APS, Figure 1d, also used to determine the valence band (VB) of FA_{0.95}CS_{0.05}PbI₃). The band gap energies (E_g) are determined from the Tauc plots, Figure 1e, obtained from UV-vis absorption spectra. The equilibrium dark Fermi levels ($E_{F,dark}$) were measured by Kelvin probe (Figure 1f). From these combined data we construct the flat band energy diagram at the HTL/FA_{0.95}CS_{0.05}PbI₃ interfaces, Figure 1f. Looking in detail at the two HTLs the HOMO level of PF8TAA shifts by 0.21 eV compared with PTAA and is accompanied by a moderate reduction of p-doping level and a negligible change in E_g (Table S1, Supporting Information).

Having interrogated the intrinsic properties of the HTLs and perovskite materials we now turn to investigate the influence of HTL on device performance. **Figure 2a** shows statistical performance data for cells prepared using each of the HTLs (also Table S3, Supporting Information). From these data it can be seen that devices prepared using PF8TAA generally outperform those utilizing PTAA. The average V_{oc} value for PTAA is 1.01 (± 0.01) V increasing to 1.05 (± 0.01) V when PF8TAA is used, resulting in an increase in PCE from 17.08 (± 0.68)% to 17.64 (± 0.75)%. The champion J-V curves for each HTL are given in Figure 2b with their corresponding External quantum

efficiency (EQE) spectra shown in Figure 2c. For PTAA, the highest measured V_{oc} was 1.02 V, resulting in a measured PCE of 18.08%. In contrast, an enhanced V_{oc} of 1.06 V was achieved in the PF8TAA system resulting in a PCE of 18.26%. All devices exhibited negligible J-V hysteresis (Figure S2; Table S4, Supporting Information). A similar trend is observed between PTAA and PF8TAA devices using MAPbI₃ as the active layer (Figure S3; Table S5, Supporting Information), where the highest measured V_{oc} increased from 1.06 V to 1.12 V and the PCE of the champion cell from 17.06% to 17.87%.

To improve our understanding of the influence of the HOMO_{HTL} on V_{oc} we employed PL spectroscopy at a range of incident light intensities for complete devices containing PTAA and PF8TAA HTLs. The PL intensity versus illumination intensity data is shown in **Figure 3a**, exhibiting similar behavior that can be described by a power law $PL_{(l)} \propto I^k$. The exponent k is determined from the slope of the fitted data, which in this case are $k_{PTAA} = 1.86$ and $k_{PF8TAA} = 1.78$. The similarity between k_{PTAA} and k_{PF8TAA} indicates that the dominant recombination mechanism in each is similar. Rather than focus on the recombination mechanisms here we shift attention to the differences between relative PL signals (PL_{rel}) and how these vary with incident light intensity. From the absolute intensity of steady-state PL, the quasi-Fermi level splitting (ΔE_F) in the bulk perovskite layer can be obtained,^[18] described by a generalized Plank's law.^[19] The relationship can be simplified when only the PL_{rel} is measured, such that $\Delta E_{F,bulk} = kT \ln(PL_{rel}) + C$, where C is a calibration factor requiring separate determination, thus we can directly correlate changes in V_{oc} with changes in PL_{rel} .^[20]

From Figure 3a several observations can be made. Most obviously the PL_{rel} for the PF8TAA devices is greater than that for PTAA at all light intensities, and that the difference is greater at low light intensities. Looking at 1 Sun intensity that is that at which the J-V characteristics were obtained, the PL_{rel} for the PF8TAA device is $\approx 100\%$ greater than that of the PTAA device indicating an increase of the $\Delta E_{F,bulk}$ by ≈ 16 meV. The difference between $\Delta E_{F,bulk}$ is much less than the measured ΔV_{oc} (80 meV). Thus we can conclude that the measured V_{oc} does not equate to the $\Delta E_{F,bulk}$ in the active layer, indicating bending of hole quasi-Fermi level ($E_{F,p}$) at the perovskite-HTL interface.^[21,22]

Figure 3b shows a semi-log plot of V_{oc} as a function of light intensity. Fitting these data allow us to obtain an ideality factor (n_{id}) that describes how V_{oc} varies with light intensity. The n_{id} values are calculated to be 1.40 and 1.54 for PTAA and PF8TAA respectively, we do not expand on the recombination mechanism information that may be extracted from such calculations, owing to their non-trivial interpretation,^[8,23,24] A rather clear trend, however, is that the higher n_{id} value for the PF8TAA device results in the V_{oc} improvements seen at higher light intensities. This is clearly observed in the data, where at an illumination intensity of 0.01 mW cm^{-2} ΔV_{oc} is 23 mV whereas at 100 mW cm^{-2} , that is 1 Sun ΔV_{oc} increases to 80 mV. By extrapolating the data in Figure 3a we can estimate the difference in PL_{rel} between PTAA and PF8TAA devices at 0.01 mW cm^{-2} to be fourfold, corresponding to ΔV_{oc} of 36 mV, this fits well with the measured data, Figure 3b, of 23 mV.

Thus, at low light intensities the changes in PL_{rel} track the changes in V_{oc} where the magnitude of the $\Delta E_{F,bulk}$ is

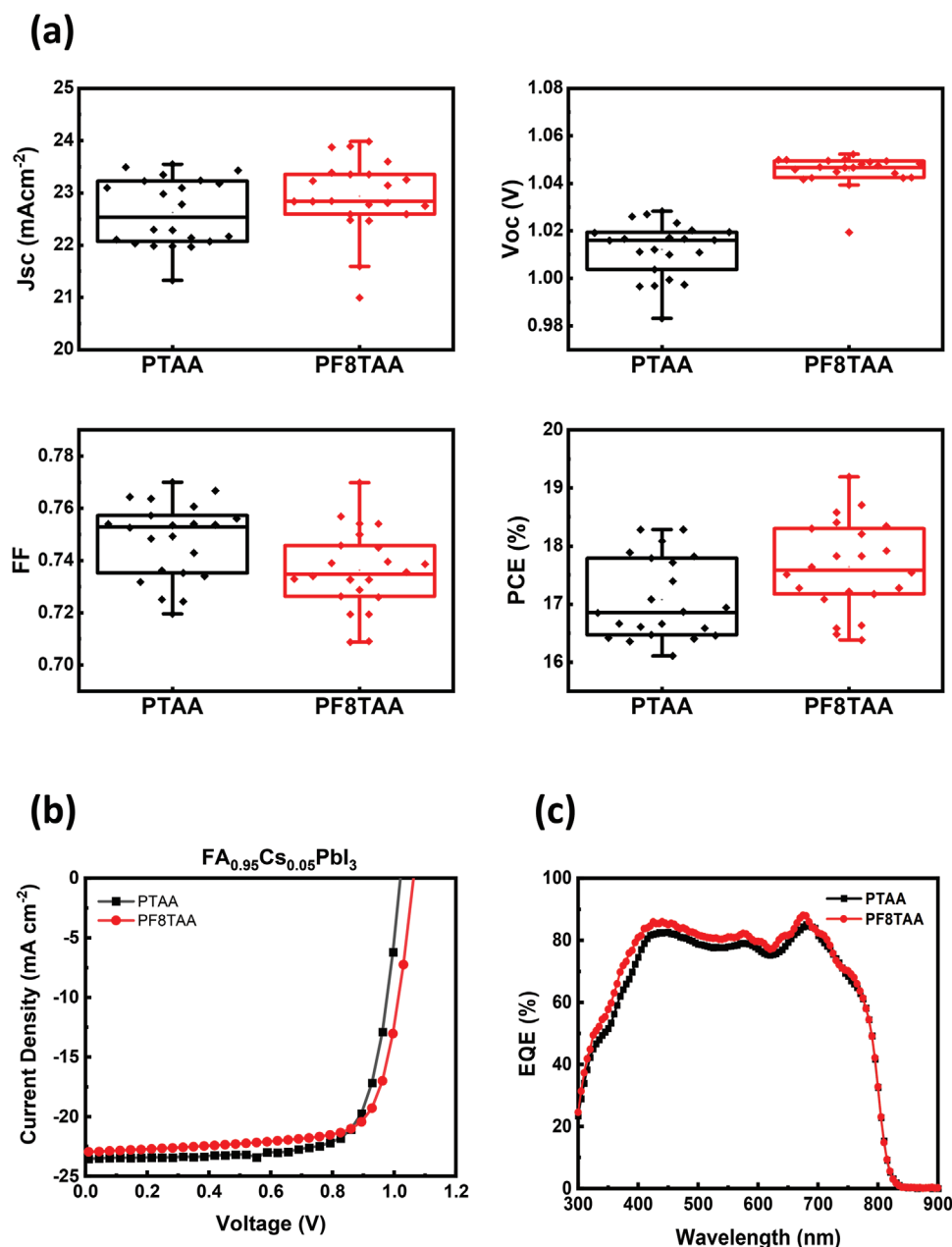


Figure 2. a) Statistical distribution of measured device parameters for PTAA and PF8TAA PSCs b) J–V curves obtained for devices with the highest V_{oc} values, c) EQE spectra of PTAA and PF8TAA PSCs.

small – resulting in a small degree of upward bending of $E_{F,p}$ between the active layer and the HTL, Figure 3c. A contrasting trend is observed at higher light intensities where the PTAA and PF8TAA devices exhibit smaller differences in $\Delta E_{F,bulk}$ but greater differences in V_{oc} . As V_{oc} measures ΔE_F between the two electrodes, the greater mismatch between V_{oc} and $\Delta E_{F,bulk}$ indicates stronger upward bending of $E_{F,p}$ in the PTAA. In such cases, Figure 3d, the V_{oc} becomes limited by the extent of upward bending of $E_{F,p}$ required to align with the HOMO_{PTAA} compared with the HOMO_{PF8TAA}. Thus, the magnitude of $\Delta E_{F,bulk}$ becomes greater as light intensity increases – whereby the $E_{F,p}$ bending at HTL/perovskite interface becomes more significant, this induces greater V_{oc} losses and we observe a larger mismatch between the V_{oc} and $\Delta E_{F,bulk}$.

In addition, time-resolved PL spectroscopy was used to probe charge extraction and recombination dynamics and correlate with device performance, Figure S4 (Supporting Information). The data from the neat perovskite films can be fitted to biexponential decay, the faster phase attributed to trap-mediated non-radiative recombination and the slower decay to the bimolecular recombination. When interfaced with our HTLs significant PL quenching is observed with both, but to a greater extent when PF8TAA is employed indicating more efficient charge transfer.^[12] This may be attributed to a reduction in surface/interfacial trap density but will also be driven by the improved band alignment.

These results highlight the limitations of V_{oc} that result from the magnitude of the energetic offset of the HOMO_{HTL} and the

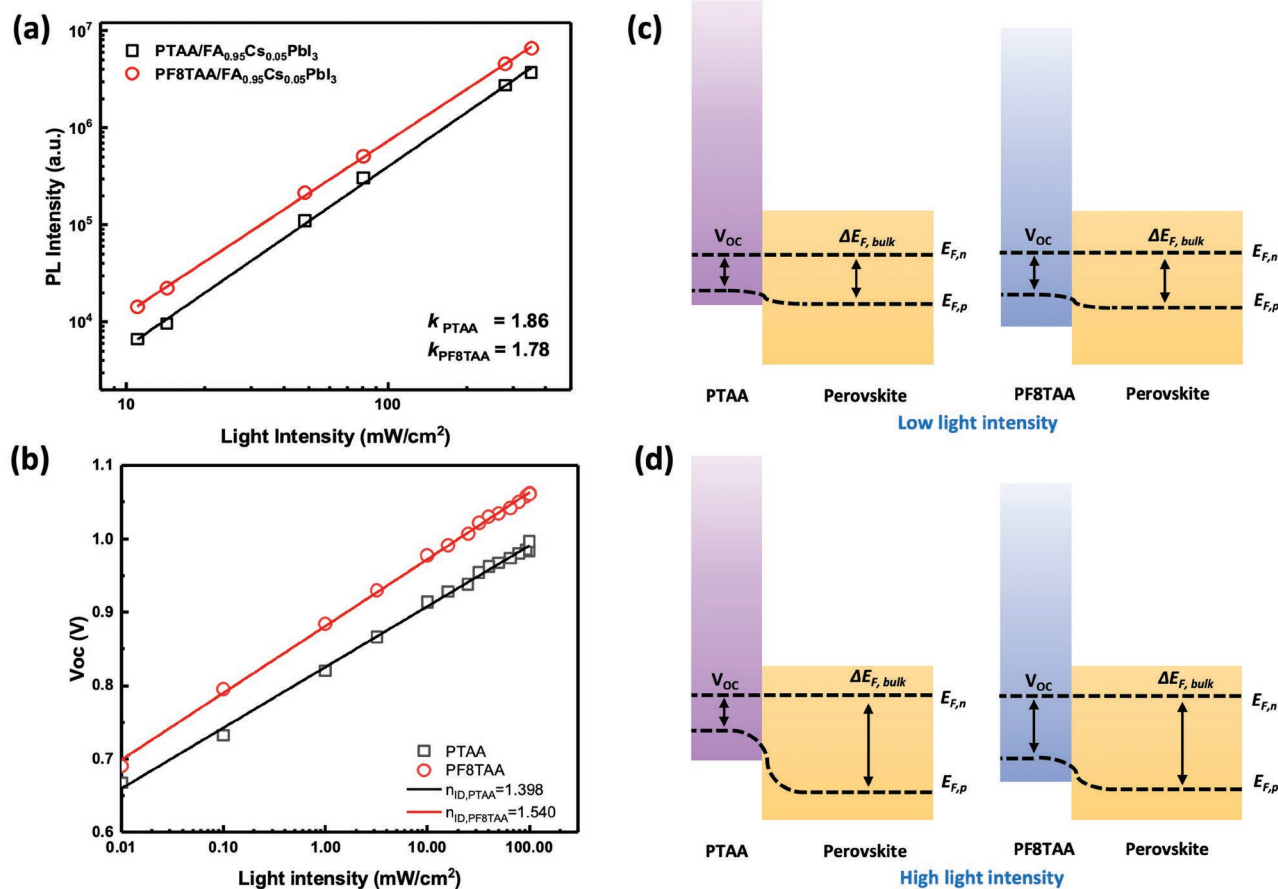


Figure 3. a) Light intensity-dependent photoluminescence measured on PTAA and PF8TAA PSCs b) Light intensity-dependent V_{oc} measured on PTAA and PF8TAA PSCs respectively, with extracted ideality factors. c,d) Schematic representations of the band diagrams at an open circuit, under (c) low light conditions and (d) high light conditions.

VB of the perovskite. This is exemplified at higher light intensities, where the value of $\Delta E_{F, bulk}$ approaches the magnitude of the perovskite E_g . This corresponds to the higher illumination levels in our case and fits the scenario of high- V_{oc} PSCs comprising high-quality perovskite layer with well passivated defects in bulk or interfaces. In the case where $\Delta E_{F, bulk}$ is much smaller than the perovskite E_g , the V_{oc} is mainly determined by $\Delta E_{F, bulk}$ and is less influenced by $H_{TL,HOMO}$. In the present work, this corresponds to lower illumination intensities and can be extended to the more general case where non-radiative recombination is a dominant factor limiting $\Delta E_{F, bulk}$. This may of course be attributed to a lack of defect passivation in the perovskite/interlayers or to high doping densities of the HTL. Therefore, the lack of correlation between $H_{TL,HOMO}$ and V_{oc} can be a common phenomenon in non-state-of-the-art PSCs having relatively low V_{oc} -to- E_g -ratio.

3. Conclusion

We have successfully fabricated and provided in-depth structural and device characterization of pin perovskite solar cells that compare the HTL performance of PTAA against that of its related co-polymer, PF8TAA. The comparable molecular

structure of these HTLs combined with their similar band gaps and doping levels allows for a focused investigation on the impact of $H_{O,HOMO}$ on device performance, more specifically V_{oc} .

Devices reliant on PF8TAA as an HTL outperform those consisting of a PTAA HTL, this is true for $FA_{0.95}Cs_{0.05}PbI_3$ and $MAPbI_3$ active layers. To better understand this behavior, we applied light-intensity dependent PL and JV measurements, through which we have made a number of significant observations. We see significant differences in the PL behavior in $FA_{0.95}Cs_{0.05}PbI_3$ thin films when interfaced with the different HTLs, where the PL_{rel} for the PF8TAA devices is greater than PTAA devices at all light intensities, more so at low light intensities. At low light intensities changes in PL_{rel} follow variations in V_{oc} – conditions where the magnitude of the $\Delta E_{F, bulk}$ is small – resulting in a small degree of upward $E_{F, p}$ bending between the active layer and the HTL. At higher light intensities devices prepared with the two HTLs exhibit less difference of $\Delta E_{F, bulk}$ however greater differences in V_{oc} . Here the V_{oc} becomes limited by the extent of upward $E_{F, p}$ bending required to align with $H_{O,PTAA}$ compared with $H_{O,PF8TAA}$. Thus, the magnitude of $\Delta E_{F, bulk}$ becomes greater as light intensity increases, and the $E_{F, p}$ bending at the HTL/perovskite interface becomes more significant, inducing greater V_{oc} losses.

Our work provides new insights into the previously unresolved issue regarding the role of HTLs' HOMO level on device V_{oc} , demonstrating that minimizing the energetic offset between the HTLs and perovskite is critical for further reducing V_{oc} losses in the pursuit of state-of-the-art perovskite solar cells.

Supporting Information

Supporting Information is available from the Wiley Online Library or from the author.

Acknowledgements

This work was supported by the Global Research Laboratory Program of the National Research Foundation (NRF) funded by the Ministry of Science, ICT & Future Planning (NRF-2017K1A1A2013153); the GIST-ICL International Collaboration R&D Centre. Additionally, the authors acknowledge the EPSRC Centre for Doctoral Training in Plastic Electronic Materials EP/L016702/1 for continued student support and training. Z.J. would like to acknowledge the China Scholarship Council (CSC) for financial support. T.J.M. would like to thank the Royal Commission for the Exhibition of 1851 for their financial support through a Research Fellowship. Y.C.C. would like to acknowledge the support of the President's Ph.D. scholarship from Imperial College London. T.D. gratefully acknowledges the Stephen and Anna Hui Scholarship (Imperial College London) for financially supporting his doctoral studies.

Conflict of Interest

The authors declare no conflict of interest.

Data Availability Statement

The data that support the findings of this study are available in the supplementary material of this article.

Keywords

interlayers, open-circuit voltage, perovskite, photovoltaic, photoluminescence

Received: August 5, 2022

Revised: October 14, 2022

Published online: December 1, 2022

[1] T. Du, S. R. Ratnasingham, F. U. Kosasih, T. J. Macdonald, L. Mohan, A. Augurio, H. Ahli, C.-T. Lin, S. Xu, W. Xu, R. Binions, C. Ducati, J. R. Durrant, J. Briscoe, M. A. McLachlan, *Adv. Energy Mater.* **2021**, *11*, 2101420.

- [2] X.-X. Gao, W. Luo, Y. Zhang, R. Hu, B. Zhang, A. Züttel, Y. Feng, M. K. Nazeeruddin, *Adv. Mater.* **2020**, *32*, 1905502.
- [3] A. K. Jena, A. Kulkarni, T. Miyasaka, *Chem. Rev.* **2019**, *119*, 3036.
- [4] C.-T. Lin, J. Lee, J. Kim, T. J. Macdonald, J. Ngiam, B. Xu, M. Daboczi, W. Xu, S. Pont, B. Park, H. Kang, J.-S. Kim, D. J. Payne, K. Lee, J. R. Durrant, M. A. McLachlan, *Adv. Funct. Mater.* **2020**, *30*, 1906763.
- [5] L. Tian, W. Zhang, H. Yu, C. Peng, H. Mao, Y. Li, Q. Wang, Y. Huang, *ACS Appl. Energy Mater.* **2019**, *2*, 4954.
- [6] W. Yan, S. Ye, Y. Li, W. Sun, H. Rao, Z. Liu, Z. Bian, C. Huang, *Adv. Energy Mater.* **2016**, *6*, 1600474.
- [7] J.-P. Correa-Baena, W. Tress, K. Domanski, E. H. Anaraki, S.-H. Turren-Cruz, B. Roose, P. P. Boix, M. Grätzel, M. Saliba, A. Abate, A. Hagfeldt, *Energy Environ. Sci.* **2017**, *10*, 1207.
- [8] T. Du, W. Xu, M. Daboczi, J. Kim, S. Xu, C.-T. Lin, H. Kang, K. Lee, M. J. Heeney, J.-S. Kim, J. R. Durrant, M. A. McLachlan, *J. Mater. Chem. A* **2019**, *7*, 18971.
- [9] M. Stolterfoht, P. Caprioglio, C. M. Wolff, J. A. Márquez, J. Nordmann, S. Zhang, D. Rothhardt, U. Hörmann, Y. Amir, A. Redinger, L. Kegelman, F. Zu, S. Albrecht, N. Koch, T. Kirchartz, M. Saliba, T. Unold, D. Neher, *Energy Environ. Sci.* **2019**, *12*, 2778.
- [10] M. Stolterfoht, C. M. Wolff, J. A. Márquez, S. Zhang, C. J. Hages, D. Rothhardt, S. Albrecht, P. L. Burn, P. Meredith, T. Unold, D. Neher, *Nat. Energy* **2018**, *3*, 847.
- [11] C.-T. Lin, W. Xu, T. J. Macdonald, J. Ngiam, J.-H. Kim, T. Du, S. Xu, P. S. Tuladhar, H. Kang, K. Lee, J. R. Durrant, M. A. McLachlan, *ACS Appl. Mater. Interfaces* **2021**, *13*, 43505.
- [12] W. Xu, T. Du, M. Sachs, T. J. Macdonald, G. Min, L. Mohan, K. Stewart, C.-T. Lin, J. Wu, R. Pacalaj, S. A. Haque, M. A. McLachlan, J. R. Durrant, *Cell Rep. Phys. Sci.* **2022**, *3*, 100890.
- [13] W. Yan, Y. Li, Y. Li, S. Ye, Z. Liu, S. Wang, Z. Bian, C. Huang, *Nano Energy* **2015**, *16*, 428.
- [14] B. Dänekamp, N. Droseros, D. Tsokkou, V. Brehm, P. P. Boix, M. Sessolo, N. Banerji, H. J. Bolink, *J. Mater. Chem. C* **2019**, *7*, 523.
- [15] C. Bi, Q. Wang, Y. Shao, Y. Yuan, Z. Xiao, J. Huang, *Nat. Commun.* **2015**, *6*, 7747.
- [16] W. Zhang, J. Smith, R. Hamilton, M. Heeney, J. Kirkpatrick, K. Song, S. E. Watkins, T. Anthopoulos, I. McCulloch, *J. Am. Chem. Soc.* **2009**, *131*, 10814.
- [17] J. Lee, H. Kang, G. Kim, H. Back, J. Kim, S. Hong, B. Park, E. Lee, K. Lee, *Adv. Mater.* **2017**, *29*, 1606363.
- [18] T. Kirchartz, J. A. Márquez, M. Stolterfoht, T. Unold, *Adv. Energy Mater.* **2020**, *10*, 1904134.
- [19] P. Würfel, W. Ruppel, *J. Lumin.* **1981**, *24–25*, 925.
- [20] T. Trupke, R. A. Bardos, M. D. Abbott, J. E. Cotter, *Appl. Phys. Lett.* **2005**, *87*, 093503.
- [21] P. Caprioglio, M. Stolterfoht, C. M. Wolff, T. Unold, B. Rech, S. Albrecht, D. Neher, *Adv. Energy Mater.* **2019**, *9*, 1901631.
- [22] S. Wheeler, F. Deledalle, N. Tokmoldin, T. Kirchartz, J. Nelson, J. R. Durrant, *Phys. Rev. Appl.* **2015**, *4*, 024020.
- [23] P. Caprioglio, C. M. Wolff, O. J. Sandberg, A. Armin, B. Rech, S. Albrecht, D. Neher, M. Stolterfoht, *Adv. Energy Mater.* **2020**, *10*, 2000502.
- [24] W. Tress, M. Yavari, K. Domanski, P. Yadav, B. Niesen, J. P. Correa Baena, A. Hagfeldt, M. Graetzel, *Energy Environ. Sci.* **2018**, *11*, 151.